 MCB, vol.4, no.3, pp.119-131, 2007

Tensorial Description of the Geometrical Arrangement of the Fibrous Molecules in Vascular Endothelial Cells

Wei Huang*

Abstract: This work presents a tensorial description of the geometrical arrangement of the cellular molecules in the vascular endothelial cells. The geometrical arrangement of the molecules is the foundation of the mechanical properties of the molecular aggregates, which are the foundation of the physical behavior of the cells and tissues. For better studying the physical behavior of the cells and tissues, the geometrical arrangement of the cellular molecules has to be described quantitatively. In this paper, a second order *molecular configuration tensor* P_{ij}^g for fibrous protein in the cells is defined for quantitative measurement. Here, the subscripts i, j refer to the coordinate axes x_1, x_2, x_3, and the superscript g refers to the kind of fibrous protein. Every molecular configuration tensor P_{ij}^g has 9 components. To give an example, the F-actin fibers in the vascular endothelial cells were studied. These molecules were stained with phalloidin and observed in a confocal microscope. Digitized images of the F-actin fibers were analyzed to determine the F-actin's molecular configuration tensor P_{ij}^g. The tensor P_{ij}^g is a simple and definitive description of a complex system of molecules which are important in the research on tissue remodeling of blood vessels. In this article, the P_{31} and P_{32} values in the P_{ij}^g tensor of F-actin fiber in the endothelial cells in rat's abdominal aorta were obtained, and the distributions of these two components in the endothelial cells were presented. The molecular configuration tensor P_{ij}^g can be applied to other fibrous proteins in the cells and to cells other than vascular endothelial cells.

Keyword: fibrous protein, F-actin, tensor

* Department of Bioengineering, University of California San Diego, La Jolla, CA 92093-0412

1 Introduction

This paper is a part of a general study of the mechanics of the cells in a blood vessel responding to the changes of blood pressure and blood flow. Vascular endothelial cells in blood vessel are exposed to dynamic stretching and shearing due to blood pressure and blood flow. In recent years, the effects of hemodynamics on the endothelial biology have become a focus of research in vascular physiology and diseases [1]. As stress and strain are imposed on the cells, the DNA and subsequently all the structural protein molecules, such as actin, microtubule, intermediate filament, etc., deform or actively rearrange themselves.

During the past decade, a growing body of evidence has indicated that the cytoskeleton plays a major role in transmitting and distributing mechanical stresses within the cell, as well as in their conversion into biochemical responses. Endothelial cells and their intracellular stress fibers, i.e., F-actin fibers, show characteristic orientations in different parts of the vasculature [2]. In the straight part of the arterial tree, both endothelial cells and their intracellular stress fibers are oriented in a longitudinal direction of an artery, which is parallel to the direction of wall shear stress and perpendicular to the direction of circumferential stretch in the artery. At arterial branches, which are sites of prevalence for atherosclerosis [3], endothelial cells and their stress fibers do not have clear patterns of orientation [4]. The roles of different shear stress and stretch patterns in endothelial cell orientation and predilection for atherosclerosis have been studied [1]. Galbraith et al. showed that the actin, tubulin, and vimentin in the vascular endothelial cells undergo remodeling to become oriented with the direction of shear flow, with a consequent align-

ment of the cell with the shear flow direction [4]. Helmke et al. were the first one to analyze the displacement of intermediate filaments in living vascular endothelial cells in response to shear stress [5]. Karlon et al. used intensity gradients in images of control and sheared endothelial cells to measure cell orientation distributions and cytoskeletal filament organization [6]. Langille et al. used abdominal aortic coarctation in rabbits to experimentally increase shear stress downstream from the coarctation by approximately twofold to study the redistribution of F-actin in the period immediately after experimental changes in shear [7]. Sipkema et al. studied the effect of cyclic alterations in axial stretch independent of flow on endothelial cytoskeletal organization in intact arteries and found that cyclic axial stretching of intact vessels under normal transmural pressure in the absence of shear stress induces within a few hours realignment of endothelial actin stress fibers toward the circumferential direction [8]. Kaunas et al. demonstrated that the stretch-induced stress fiber orientation is a function of the interplay between Rho pathway activity and the magnitude of stretching [9]. Hu et al. measured displacements and computed stresses in the cytoskeleton of a living cell plated on extracellular matrix molecules that arise in response to a small, external localized oscillatory load applied to transmembrane receptors on the apical cell surface, and found that mechanical forces are transferred across discrete cytoskeletal elements over long distances through the cytoplasm in the living adherent cell [10]. Other advanced methods to measure the spatial organization of the cytoskeleton in cells for investigating the effects of hydrodynamic forces in cells were developed [11]. However, how do these cellular molecules affect the mechanical properties of the cells in health and diseases is still largely unknown.

In studying the physiology of man, it is necessary to understand the human anatomy as a preliminary. In studying the mechanics of the molecules in a vascular cell, it is necessary to understand the geometry of the individual molecules and the geometrical structure of the aggregation of the molecules in the vessel wall. The geometry is the foundation of the mechanical properties of the molecular aggregates. The mechanical properties of the molecular aggregates are the foundation of the physical behavior of the cells and tissues. Following this reasoning, it is important to clarify the geometric structure of the aggregation of these molecules. The purpose of the present article is to show that the tensor language is helpful to describe the geometric distribution of fibrous molecules in the cells. F-actin fibers in vascular endothelial cells are examined in this paper. Clearly, the concept and technique can be applied to analyze any fibrous molecules in biology.

2 Definition of Molecular Configuration Tensor P_{ij}^g

In Fig. 1A, the upper figure shows a blood vessel with flow, the lower figure shows a schematic drawing of the endothelium. A Cartesian coordinate system is shown with x_1-axis parallel to the direction of blood flow, x_3-axis perpendicular to the basal lamina, and x_2-axis normal to x_1 and x_3. In Figure 1B, a plan view of the endothelial cells of a rat's abdominal aorta in a plane perpendicular to the endothelium (x_3 axis) is shown.

The inner diameter of this aortic section, measured with an Olympus light microscope (Model: AH-2), was 1.05 ± 0.22 mm (mean $\pm$ standard deviation). Examined under a confocal microscope, the endothelium is located first. When the projected boundaries of endothelial cells are barely seen, that boundary is said to be at $x_3 = 0$ μm. By stepping the objective in the direction of the x_3-axis, the endothelial cells and F-actin fibers can be examined. The optical section image in Fig.1B was taken at $x_3 = 1.4$ μm. The F-actin fibers and the nuclei in the cells were stained. The thick bright lines are the boundaries of the endothelial cells. Cells A, B, C are shown. The thin bright lines inside the cells are F-actin fibers. The geometric distribution of the F-actin fibers in the cells can be quantitatively described by the P_{ij}^g tensor of F-actin fibers defined below.

Figure 2 illustrates the steps to describe the geometric distribution of the actin fibers in a cell. The fibers are illustrated in Fig. 2A. Consider a unit cube in Fig. 2B. Superpose it on the fibers of

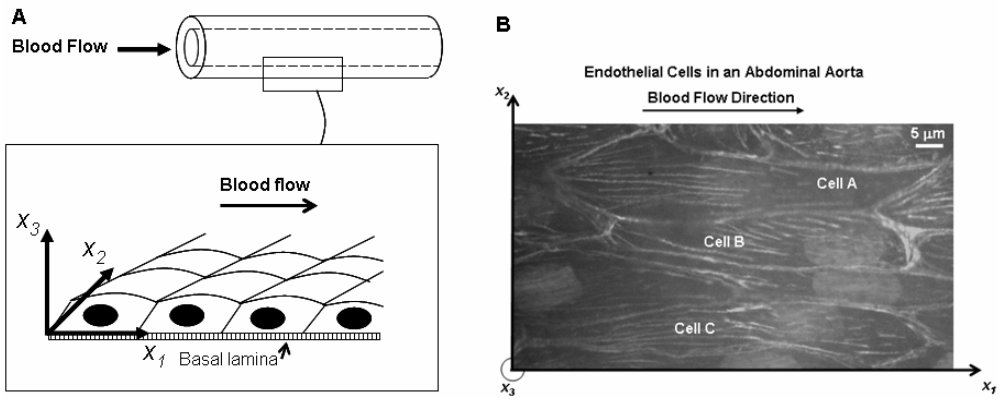

Figure 1: A schematic drawing of a blood vessel with the direction of blood flow in the upper figure, and a magnified schematic drawing of the endothelium with a longitudinal cross section in the front in the lower figure. A Cartesian coordinate system with x_1-axis parallel to the direction of blood flow, x_3-axis perpendicular to the basal lamina, and x_2-axis normal to x_1 and x_3 is used as references to label the endothelium. (B) A plan view of the endothelial cells in a rat's abdominal aorta in a plane perpendicular to the endothelium (x_3 axis). The inner diameter of the aortic section for examination was 1.05 ± 0.22 mm. The optical section image in Fig. 1B was taken at 1.4 μm along the thickness of the cell (x_3-axis) while at 0 μm the boundaries of the endothelial cell were barely seen in a confocal microscope. The F-actin fibers and nuclei in the cells were stained. The thick bright lines are the boundaries of the endothelial cells. The thin lines inside the cells are the F-actins. The F-actin fibers appear complex. Three projected cells are enclosed with cell boundaries, and labeled as Cell A, Cell B, and Cell C. Bar length: 5 μm.

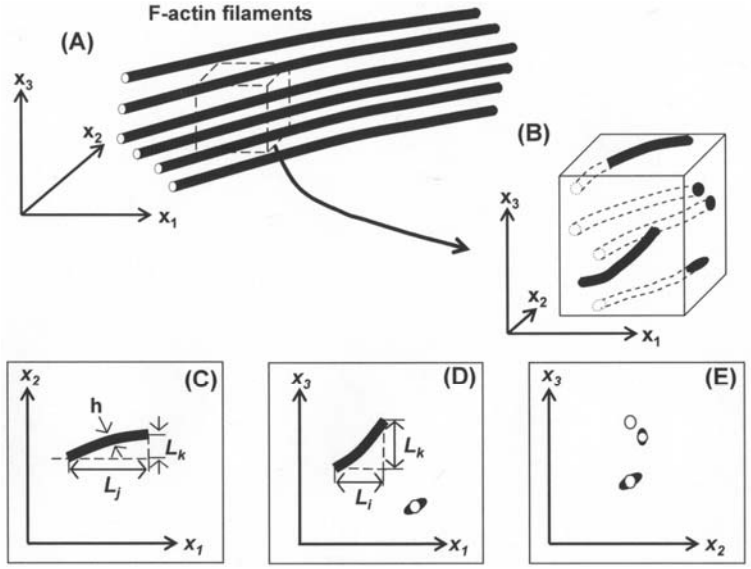

Figure 2: A scheme to describe how to measure the P_{ij}^{g} tensors of fibrous proteins. See details in Section 2.

Fig. 2A. Photograph the fibers cut by the six faces of the cube. With a rectangular Cartesian frame of reference with coordinates (x_1, x_2, x_3), i.e., x_i, with $i = 1, 2,$ or 3, a plane normal to the x_i axis cuts the cells in the $x_j - x_k$ plane, $j, k = 1, 2,$ or 3. A fiber which appears as a circular spot in the $x_j - x_k$ plane is interpreted as perpendicular to the $x_j - x_k$ plane, i.e., lying in the direction of x_i axis. A spot that is elliptical is interpreted as a fiber that cuts the $x_j - x_k$ plane at an angle: In that case a circle is counted with radius equal to the minor axis of the ellipse as the normal component. In the $x_j - x_k$ plane shown in Figs. 2C, 2D, and 2E, the length of each fiber projected onto its rectangular components L_j, L_k can be resolved. Let the thickness of the fiber be h. The diameter of the dots is also h. For an elongated dot, a circle of diameter h is treated as a dot and the length of (major – minor) diameter as L_j, L_k. Then, on summing over all segments in an area A (of the rectangle of the figures), the numbers can be computed:

$$\begin{aligned} P^g_{ii} &= \frac{1}{A}\sum \text{area of the dots}, \\ P^g_{ij} &= \frac{1}{A}\sum hL_j, \\ P^g_{ik} &= \frac{1}{A}\sum hL_k. \end{aligned} \tag{1}$$

If these numbers were known for all $i, j, k = 1, 2, 3$, the following matrix may be written as P^g_{ij}:

$$\begin{bmatrix} P_{11} & P_{12} & P_{13} \\ P_{21} & P_{22} & P_{23} \\ P_{31} & P_{32} & P_{33} \end{bmatrix} = P^g_{ij}, \tag{2}$$

g refers to the kind of fibrous proteins. P^g_{ij} is a second order tensor, and is called the *molecular configuration tensor* P^g_{ij} for the fibrous protein g. In the present article, g refers to the F-actin fiber.

3 Materials and Methods

3.1 Tissue Sample Preparation

Sprague Dawley rats were anesthetized with pentobarbital (50 mg/kg body weight). A bolus of normal saline with 1000 U/kg body weight of heparin (1000 U/ml) was injected. Before blood vessel perfusion, a bolus of normal saline with 1000 U/kg body weight of heparin (1000 U/ml) was injected through a cannula. The abdominal aorta was fixed *in situ* by vascular perfusion of 4 percent formaldehyde in 0.1 M physiological saline buffer (PBS) for 1 hour under a perfusion pressure of 80 mm Hg and a draining pressure of 0 mm Hg at the inferior vena cava. The aorta was cut and transferred to a container containing PBS for isolating abdominal aorta under an Olympus SZH zoom stereo microscope. To protect the endothelial cells, keeping the in-situ length of the segment and never jerking it either way at any time are extremely important. Our animal protocol has been reviewed and approved by the University of California, San Diego Committee on Animal Research, in conformity with the Guide for the care and Use of Laboratory Animals (NIH, 1996).

The formaldehyde-fixed blood vessels were cut into strips of appropriate sizes with orientation marked by referring to the blood flow direction, and the endothelium for fluorescent staining.

3.2 Fluorescent Staining the Endothelial Cells in the Blood Vessel

The vascular strips of rat's abdominal aorta were washed in PBS, incubated with a mixture of 5 U/ml Alexa Fluor 488 phalloidin (Molecular Probes, Eugene, OR), 1 percent bovine serum albumin (Sigma-Aldrich, St. Louis, MO), 0.5 percent triton x-100 (Sigma-Aldrich), and PBS for 1 hour at 37^{o}C, and washed three times in PBS (5 minutes each time); then stained with To-Pro-3 (Molecular Probes, concentration 1:500) for 20 min at room temperature, and washed three times in PBS (5 minutes each time). Phalloidin stains F-actin fibers in the endothelial cells [12]. To-Pro-3 stains nuclei in the cells [13]. Strips without phalloidin and To-Pro-3 were used as controls.

The fluorescence stained strips were placed on microscope slides (Superfrost Plus GOLD) with the endothelium facing up, and mounted with Pro-Long Gold antifade regent (Molecular Probes). A #1.5 micro cover glass (Thamos Scientific) was placed on top of the endothelium, and the edges of the cover glass were sealed with nail polish.

3.3 Confocal Microscopy Examination

A confocal scanning microscope (Model 10, Yokogawa, Tokyo, Japan), with a set of fluorescence filters (Excitation: 488 nm, Emission: 525 nm, Band Width: 50 nm), was used. A 60× 1.45 NA plan apo oil immersion objective was used. The refraction index of the immersion oil was 1.516. The calibration value for our set-up was 9.13 pixels/μm. The thickness of an optical section was 0.2 μm. By stepping the objective through the thickness of the specimen in the direction of the x_3-axis that was perpendicular to the endothelium, the endothelium and the smooth muscle layer were identified. The 2-dimensional images in x_3-axis were taken with one of the image edges perpendicular to the blood flow direction in the blood vessel. Fluorescent images were taken in successive planes, and captured with a Hamamatsu digital camera (model: ORCA-ER, Hamamatsu Photonics, Hamamatsu, Japan). Images were taken for the strips without fluorescence staining to be used as controls. Digitized images were acquired using the Simple PCI imaging software (Compix Inc., Cranberry Township, Pennsylvania) and saved in a computer for image analysis.

3.4 Measuring the Geometric Distribution of the F-actin Fibers in the Cells

The digitized images were analyzed and measured with MetaMorph Imaging system (Version: 6.3 r2, Universal Imaging Corporation, Downingtown, PA). In analyzing the images, all F-actin fibers were assumed as vectors going from left to right. The cell images in the computer yielded data on the orientation θ, width h, and length L of F-actin fibers in the cells in the plan view. Based on these measurements, the values of P_{31}, P_{32} in the P_{ij}^g tensor of F-actin in the endothelial cells were computed by Eq. (1).

4 Results

4.1 Cell Morphological Parameters

The projected cell boundaries were traced manually with MetaMorph Imaging system for determining the cell area, cell perimeter, and cell shape index. A *shape index* is computed by the following formula: *shape index = (4π×cell area)/(cell perimeter)*^{2}. For a circular cell, the shape index equals 1; for a highly elongated cell, the shape index approaches zero. The cell height and cell width of the projected cells were measured. The cell width is defined as the maximal horizontal length of the projected cell inside the boundaries, which is parallel to the x_1-axis. The cell height is defined as the maximal vertical length of the projected cell inside the boundaries, which is parallel to the x_2-axis. Table 1 summarizes the projected cell area, perimeter, shape index, height, width of Cell A, Cell B, and Cell C shown in Fig. 1B.

4.2 Values of P_{31}, P_{32} Measured in the Areas of Different Shapes, Sizes, and Locations within an Endothelial Cell

To determine the cellular stress under specific boundary conditions, the P_{ij}^g tensors of all the proteins in the cell are needed. Figure 3 illustrates how the P_{ij}^g tensor of F-actin fibers in the endothelial cell, Cell A of Fig. 1B, can be measured. In each selected area, data on the orientation θ, width h, and length L of F-actin fibers in the Cell A were collected by using the MetaMorph Imaging system, and the values of P_{31}, P_{32} were computed by Eq. (1).

Fig. 3A shows the measurements of P_{31}, P_{32} in a projected endothelial cell, Cell A. The thick bright lines are the cell boundaries, and the thin bright lines in the cell are F-actin fibers. In Fig. 3B, three concentric circles were drawn in Cell A for the measurements of P_{31} and P_{32}. Their diameters were 11 μm (Circle 1), 5.5 μm (Circle 2), and 2.75 μm (Circle 3), respectively. In Circle 1, P_{31} = 0.14, P_{32} = 0.012; in Circle 2, P_{31} = 0.17, P_{32} = -0.003; in Circle 3, P_{31} = 0.24, P_{32} = 0.0081. The values of P_{31} and P_{32} are different in these three different circles.

As shown in Figure 3C, in another location of Cell A, three concentric circles were drawn. The values of P_{31} and P_{32} in these 3 circles are: P_{31} = 0.16, P_{32} = -0.015 in Circle 1 (diameter: 11 μm); P_{31} = 0.15, P_{32} = -0.013 in Circle 2 (diameter: 5.5 μm); and P_{31} = 0.25, P_{32} = -0.010 in Circle 3 (diameter: 2.75 μm). In Fig. 3C, the values of P_{31}

Table 1: The morphological parameters of the projected endothelial cells in Fig. 1B

	Cell Area (μm^2)	Perimeter (μm)	Shape Index	Cell Width (μm)	Cell Height (μm)
Cell A	578	146	0.34	68	16
Cell B	362	112	0.35	52	10
Cell C	428	150	0.24	71	11

Note The cell width, parallel to the x_1-axis, is the maximal horizontal length of the projected cell inside the boundaries. The cell height, parallel to the x_2-axis, is the maximal vertical length of the projected cell inside the boundaries. shape index $= (4\pi \times \text{cell area})/(cell parameter)^2$. The shape index equals 1 for a circular cell, and approaches zero for a highly elongated cell.

Table 2: Variations of P_{31}, P_{32} values in the molecular configuration tensor P^g_{ij} of F-actin fibers measured in the areas of different shapes, sizes, and locations within an endothelial cell as shown in Fig. 3

	Shape	Area (μm^2)	Measured Objects	P_{31}	P_{32}
Figure 3A	Cell A	578	28	0.074	-0.0017
Figure 3B	Circle 1	94	12	0.14	0.012
	Circle 2	24	5	0.17	-0.0030
	Circle 3	6	3	0.24	0.0081
Figure 3C	Circle 1	94	13	0.16	-0.015
	Circle 2	24	7	0.15	-0.013
	Circle 3	6	3	0.25	-0.010
Figure 3D	Rectangle 1	165	20	0.17	-0.0071
	Rectangle 2	41	6	0.16	0.010
	Rectangle 3	10	3	0.29	0.039
	Rectangle 4	2	2	0.29	0.069
Figure 3E	Square 1	77	11	0.14	0.0090
	Square 2	19	4	0.19	0.023
	Square 3	5	1	0.13	0.025
Figure 3F	Square 1	77	11	0.16	-0.015
	Square 2	19	6	0.20	-0.036
	Square 3	5	1	0.086	-0.027
Figure 3G	Square 1	77	11	0.16	-0.015
	Square 2	19	6	0.26	-0.023
	Square 3	5	2	0.23	-0.048

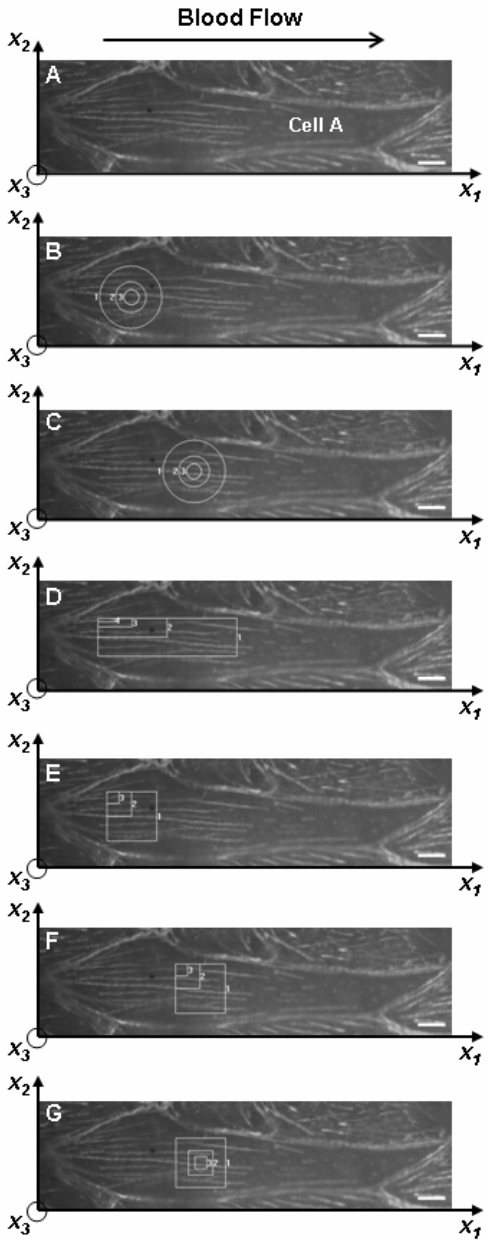

Figure 3: Values of P_{31}, P_{32} in the areas of different shapes, sizes, and locations within an endothelial cell. In (A), the measurements were made within an endothelial cell, Cell A. In (B) and (C), the measurements were made in three concentric circles of different diameters within Cell A in different locations. In (D), the measurements were made in four rectangular boxes of different areas within Cell A. In (E)-(G), the measurements were made in the squares of different areas and different locations within Cell A. The values of P_{31} and P_{32} collected are summarized in Table 2. Bar length: 5 μm.

and P_{32} are different in three different circles. The differences of P_{31} and P_{32} values between two locations within Cell A are obvious; it indicates that the geometric distribution of F-actin fibers within a cell can be described by the P^g_{ij} tensor. In Fig. 3D, the measurements were made in four rectangular areas within Cell A. The values of P_{31} and P_{32} are: P_{31} = 0.17, P_{32} = -0.0071 in Rectangle 1 (area: 165 μm^2); P_{31} = 0.16, P_{32} = 0.010 in Rectangle 2 (area: 41 μm^2); P_{31} = 0.29, P_{32} = 0.039 in Rectangle 3 (area: 10 μm^2); and P_{31} = 0.29, P_{32} = 0.069 in Rectangle 4 (area: 2 μm^2). The differences of P_{31} and P_{32} values in four different rectangular areas within Cell A are found. Figs. 3E-3G illustrate the selected squares for the measurements of P_{31} and P_{32} within Cell A. Each figure has three squares, and their areas are: 77 μm^2 (Square 1), 19 μm^2 (Square 2), and 5 μm^2 (Square 3), respectively. In Figs. 3E and 3F, all squares share the top-left corner. In Fig. 3G, three concentric squares are used. The differences of P_{31} and P_{32} values in different squares and locations within Cell A are found.

The values of P_{31} and P_{32} in the areas of different shapes, sizes, and locations within an endothelial cell in Fig. 3 are summarized in Table 2. As shown in Table 2, more objects of F-actin fibers were measured in a bigger area. In the smaller areas, only 1 or 2 objects were measured. The variations of P_{31} and P_{32} values are found.

4.3 Distributions of P_{31}, P_{32} Values in an Endothelial Cell

The distribution of F-actin fiber in an endothelial cell was analyzed in different regions of the cell, and described by the P^g_{ij} tensor of F-actin fiber as shown in Fig. 4. In every panel of Fig. 4, the boundaries of an endothelial cell, which is labeled as Cell A in Fig. 1B, are outlined with solid black lines. The cell is divided into 2, 4, 8, 16, or 30 regions, respectively, by dashed lines along its width and height. The width of a cell is defined as the maximal horizontal length of the cell, while the height of a cell is the maximal vertical length of the cell. The width of Cell A is 68 μm, while its height is 16 μm. The cell is divided into 2 regions by drawing a vertical line through the center

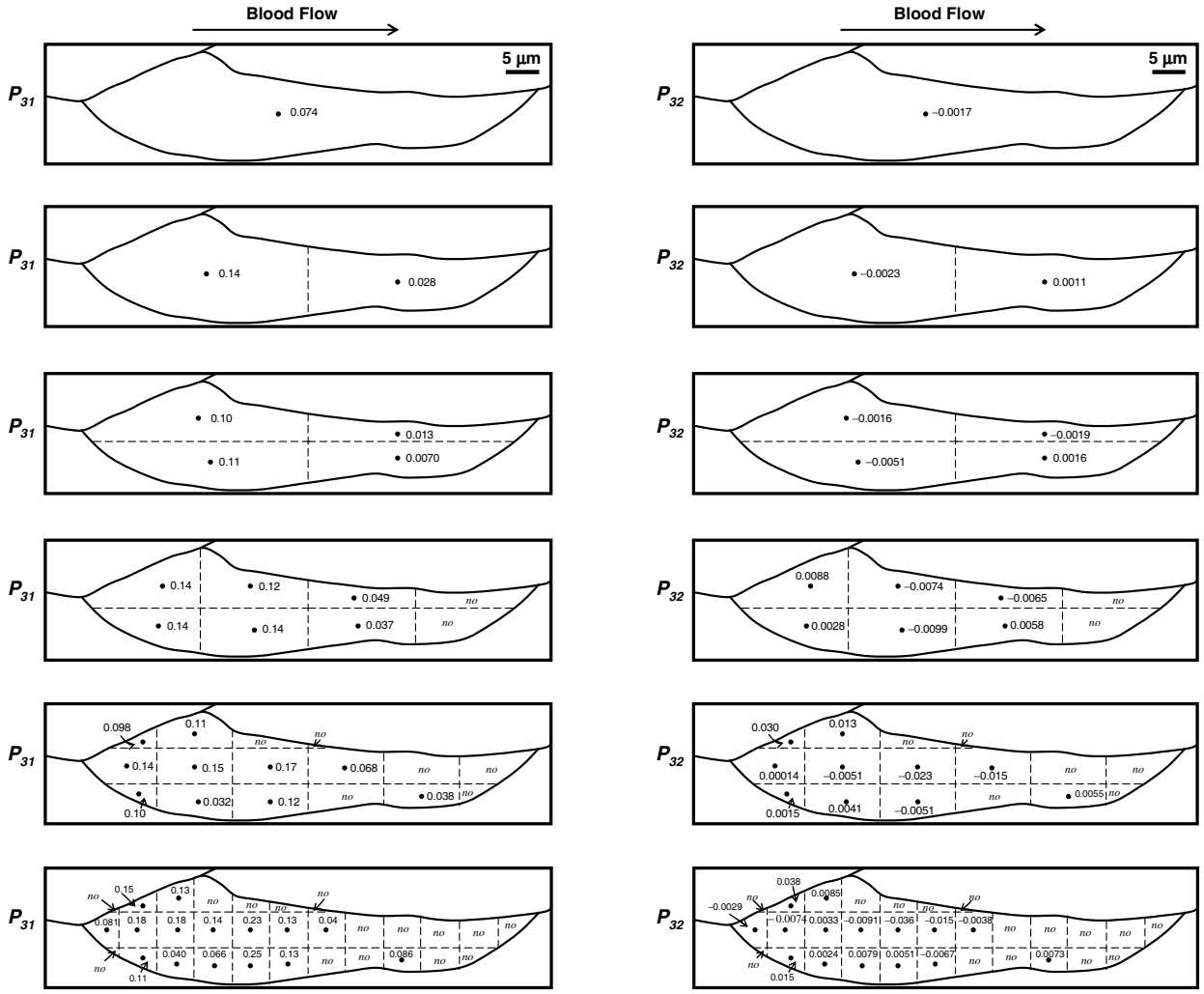

Figure 4: The distributions of P_{31} and P_{32} values in the molecular configuration tensor P^g_{ij} of the F-actin fibers in an endothelial cell. In every panel, the boundaries of an endothelial cell, which is labeled as Cell A in Fig. 1B, are outlined with solid black lines. The cell is divided into 2, 4, 8, 16, or 30 regions, respectively, by dashed lines along its width and height. The solid black dot "•" is the centroid of a region. In every region, the value of P_{31} or P_{32} is plotted next to the centroid. The regions without any measurement of F-actin fibers are marked by "*no*". Bar length: 5 μm (for all panels).

of its width, 4 regions by drawing a vertical line through the center of its width and a horizontal line through the center of its height, 8 regions by drawing a horizontal line through the center of its height and dividing its width into 4 equal lengths with 3 vertical lines, 16 regions by dividing cell height into 3 equal lengths with 2 horizontal and dividing its width into 6 equal lengths with 5 vertical lines, and 30 regions by dividing cell height into 3 equal lengths with 2 horizontal and dividing its width into 12 equal lengths with 11 vertical lines.

In every region, its boundaries were traced manually with MetaMorph Imaging system, area was measured, and centroid was computed. F-actin fibers in every region were measured by using the MetaMorph Imaging system to obtain the data on the orientation θ, width h, and length L of F-actin fibers. Based on these measurements, the values of P_{31}, P_{32} in the P^g_{ij} tensor of F-actin fibers in the vascular endothelial cell in rat's abdominal aorta and in the different regions of the cell were com-

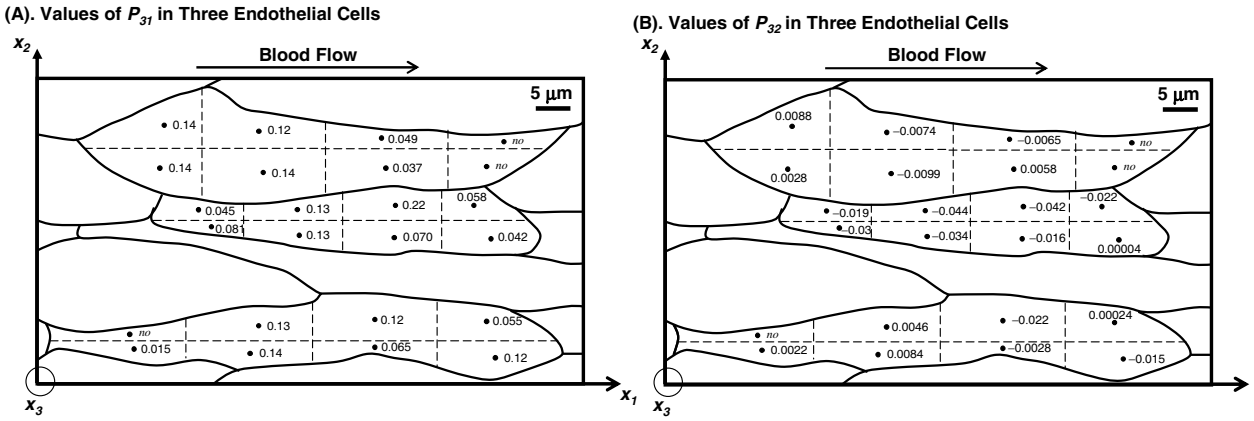

Figure 5: Variations of the P_{31} (A) and P_{32} (B) values in three endothelial cells on the same optical view. The solid black lines are the cell boundaries of the vascular endothelial cells shown in Fig. 1B. Every cell is divided into 8 regions by dashed lines along its width and height. In every region, the solid black dot "•" is the centroid of a region, and the value of P_{31} or P_{32} is plotted next to the centroid. "*no*" stands for no measurement of F-actin fibers in a selected region. Bar length: 5 μm (for all panels).

puted by Eq. (1). The values of P_{31} are presented on the left column in Figure 4, while the values of P_{32} are on the right column. In all measurements, the values of P_{33} are 0. In every panel of Fig. 4, the solid black lines are the cell boundaries of Cell A. The value of P_{31} or P_{32} is plotted next to the solid black dot "•" that is the centroid of a region. In the regions without any measurement of F-actin fibers, "*no*" is plotted. When the cell is divided into 8 regions as shown in Figure 4, no measurement of F-actin fibers was made in two regions. When the cell is divided into 16 or 32 regions, the numbers of "no measurement" regions are increased.

4.4 Values of P_{31}, P_{32} in Different Endothelial Cells on the Same Plan View

The optical section image of endothelial cells in Fig. 1B was taken at 1.4 μm through the thickness of the endothelium along the x_3-axis. The F-actin fibers and nuclei in the cells were stained. The thick bright lines are the boundaries of the endothelial cells. Three projected cells are shown to be enclosed with cell boundaries in the plan view, and labeled as Cell A, Cell B, and Cell C, respectively. In Figure 5, the solid black lines are the cell boundaries of the projected endothelial cells in Fig. 1B. The analysis is focused on the cells of A, B, and C. Every cell in Fig. 5 is divided into 8 regions by dashed lines along its width and height. The width and height of Cell A, Cell B, and Cell C are listed in Table 1. A cell is divided into 8 regions by dividing its height into 2 equal lengths with a horizontal line, and its width into 4 equal lengths with 3 vertical lines as shown in Fig. 5.

In every region of a cell, its boundaries were traced manually with the MetaMorph Imaging system, the area was measured, and the centroid was computed. F-actin fibers in every region were measured by using the MetaMorph Imaging system to obtain the data on the orientation θ, width h, and length L of F-actin fibers. Based on these measurements, the values of P_{31}, P_{32} in the different regions of the cell were computed by Eq. (1). In all measurements, the values of P_{33} are 0. The values of P_{31} in all regions of Cell A, Cell B, and Cell C are presented in Fig. 5A, while the values of P_{32} are presented in Figure 5B. Solid black lines are the cell boundaries. Each cell is divided into 8 regions by dashed lines. The solid black dot "" is the centroid of a region. In every region, the value of P_{31} or P_{32} is plotted next to the centroid. In the regions without any measurement of F-actin fiber, the region is marked by "*no*". The results show the geometric distribution of F-actin fibers in the endothelial cells quantitatively in a plan view.

4.5 Variations of P_{31}, P_{32} Values in Endothelial Cells through the Thickness of the Cells

Figure 6 shows a series of optical section images through the thickness of the fluorescence stained endothelial cells along the x_3-axis. During examination by the confocal microscope, the endothelium is located first, and the media layer is second. The optical section was set to be at 0 μm when the projected boundaries of endothelial cells were barely seen. By stepping the objective through the thickness of the specimen by an increment of 0.2 μm in the x_3-axis that is perpendicular to the endothelium, the endothelial cells and the F-actin became clear. Beyond the optical section at 1.6 μm, the endothelial cells and the F-actin fibers in the endothelial cells became unclear, and mixed with the F-actin fibers in the vascular smooth muscle cells. Figure 6A-6D show the geometrical distribution of the endothelial cells and F-actin fibers in the optical sections at x_3 = 1.0 μm (A), 1.2 μm (B), 1.4 μm (C), and 1.6 μm (D), respectively. The F-actin fibers and nuclei in the cells were stained. The thick bright lines are the boundaries of the endothelial cells.

Three projected cells are shown to be enclosed with cell boundaries in the plan view, and labeled as Cell A, B, and C, respectively. Cells A, B, and C were each divided 8 regions by drawing a horizontal line through the center of its height and dividing its width into 4 equal lengths with 3 vertical lines, as shown in Fig. 5. The width and height of Cells A, B, and C are listed in Table 1. For computing the values of P_{31}, P_{32} in different regions of the cells, F-actin fibers in every region were measured by using the MetaMorph Imaging system to obtain the data on the orientation θ, width h, and length L of F-actin fibers. In all measurements, the values of P_{33} are 0. Table 3 summarizes the values of P_{31} and P_{32} in 8 different regions of Cells A, B, C on four different optical sections. In the table, "*no*" stands for no measurement of F-actin fiber in the selected region.

As shown in Fig. 6, the geometric distribution of F-actin fibers in the endothelial cells is complex, and the patterns in different optical sections are different. The P^g_{ij} tensor of F-actin tensor provides a quantitative method for describing the different

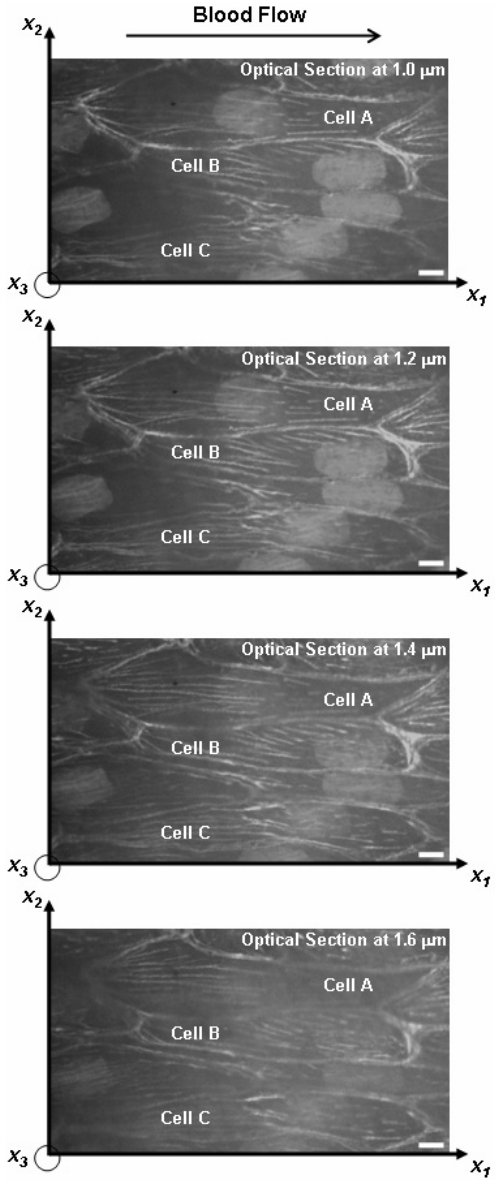

Figure 6: A series of optical section images of the endothelial cells at 1.0, 1.2, 1.4, and 1.6 μm along the thickness of the cells (x_3-axis). The F-actin fibers and nuclei in the endothelial cells were stained. The thick bright lines are the borders of the endothelial cells. The thin lines inside the cells are the F-actins. The values of P_{31} and P_{32} in the endothelial cells in different optical sections are summarized in Table 3. Bar length: 5 μm (for all panels).

Table 3: Variations of P_{31}, P_{32} values in the P_{ij}^g tensor of F-actin fibers measured in the endothelial cells of Cell A, Cell B, Cell C on the optical sections at 10, 12, 14, and 16 μm, which are shown in Fig. 6. Each cell was divided into 8 regions.

		Optical Section at 16 μm		Optical Section at 16 μm		Optical Section at 16 μm		Optical Section at 16 μm	
		P_{31}	P_{32}	P_{31}	P_{32}	P_{31}	P_{32}	P_{31}	P_{32}
	Region 1	0.010	-0.0015	0.044	-0.0052	0.14	0.0088	0.12	0.017
	Region 2	0.019	-0.0031	0.15	0.0023	0.12	-0.0074	0.095	0.0018
	Region 3	0.046	-0.010	0.063	-0.019	0.049	-0.0065	*no*	*no*
Cell A	Region 4	*no*	*no*	0.043	-0.0095	*no*	*no*	*no*	*no*
	Region 5	0.036	-0.0012	0.079	0.0038	0.14	0.0028	0.041	-0.0036
	Region 6	0.084	-0.0059	0.23	0.0039	0.14	-0.0099	0.0063	-0.00082
	Region 7	0.094	0.00037	0.15	-0.0072	0.037	0.0058	*no*	*no*
	Region 8	0.015	-0.0013	0.069	-0.015	*no*	*no*	*no*	*no*
	Region 1	0.016	-0.0055	0.050	-0.021	0.045	-0.019	*no*	*no*
	Region 2	0.13	-0.033	0.17	-0.036	0.13	-0.044	0.041	-0.021
	Region 3	0.12	-0.028	0.20	-0.047	0.22	-0.042	0.053	-0.016
Cell B	Region 4	0.019	-0.0059	0.083	-0.020	0.058	-0.022	0.040	-0.0080
	Region 5	0.073	-0.023	0.070	-0.024	0.081	-0.030	0.047	-0.014
	Region 6	0.19	-0.035	0.17	-0.030	0.13	-0.034	0.011	-0.0056
	Region 7	0.016	-0.0044	0.035	-0.0071	0.070	-0.016	0.082	-0.00007
	Region 8	*no*	*no*	*no*	*no*	0.042	0.00004	0.095	-0.033
	Region 1	*no*	*no*	*no*	*no*	*no*	*no*	*no*	*no*
	Region 2	0.064	0.0013	0.12	-0.00044	0.13	0.0046	*no*	*no*
	Region 3	0.059	-0.014	0.13	-0.022	0.12	-0.022	0.041	-0.011
Cell C	Region 4	0.042	0.00054	0.036	0.0039	0.055	0.00024	0.019	0.0051
	Region 5	0.030	0.0028	0.050	0.0044	0.015	0.0022	*no*	*no*
	Region 6	0.023	0.0025	0.083	0.0010	0.14	0.0084	*no*	*no*
	Region 7	0.038	-0.0032	0.077	-0.00006	0.065	-0.0028	0.050	-0.0055
	Region 8	0.034	-0.00023	0.084	-0.010	0.12	-0.015	0.13	-0.0055

Note *no*, no measurement was made in the selected region.

patterns of the geometric distribution of F-actin fibers in the endothelial cells as shown in Table 3.

5 Discussion

F-actin fiber in vascular endothelial cells was chosen as an example for the development and evaluation of our quantitative measure. The experimental methods of measuring P_{ij}^g tensors developed in the present article can be applied to study any fibrous proteins in other cells. F-actin fiber is one of the important cytoskeletons in the endothelial cells, and transduces extracellular forces into stresses in the cell interior [7-8, 10-11, 14]. In the present study, the P_{31} and P_{32} values in the P_{ij}^g tensor of F-actin fiber in the individual vascular endothelial cells were determined. The other values in the P_{ij}^g tensor, the influence of the nuclei in analyzing the geometrical distribution of fibrous proteins in the vascular endothelial cells, the P_{ij}^g tensor in different vascular cells and in different blood vessels, and the changes of the P_{ij}^g tensor in vascular remodeling are under investigations. The P_{ij}^g tensor provides us a tool to study the cellular molecules in the tissue remodeling of blood vessels.

In this paper, the reason for using rectangles, circles and squares as boundaries for studies is to determine whether the molecular configuration ten-

sor P_{ij}^g can be applied for quantitative measurement to different boundaries or not. As shown in Figs. 3-5, Table 2, and Table 3, the P_{ij}^g tensor can be used to describe the geometric distribution of the molecules in the areas of different shapes (rectangle, circle, and square), sizes, and locations within a cell. When applying the P_{ij}^g tensor in different areas within an endothelial cell, the values of P_{31} andP_{32} in different areas varied. The variations of the P_{ij}^g tensor within a single cell remind us the importance of stress and strain analysis in the cells.

The biomechanics of tissue remodeling needs new input at the molecular level for expressing the mechanics of the molecules in a constitutive equation of the cells, which relates the stress, strain, molecular configuration, and their history. Since the stress and strain are expressed in tensor forms in every constitutive equation, the molecular geometry has to be expressed in tensor form too. However, the tensor form of the geometry of the molecules does not exist in literature. In the present paper, the molecular configuration tensor P_{ij}^g for fibrous protein in the cells is defined. Constitutive equations relate stress to strain [15]. Experimental determination of the constitutive equation of blood vessels has a huge literature [15-16]. However, so far none of the existing constitutive equations deals explicitly with the changing molecular configurations in the cells. It is well known that in any valid constitutive equation every term in the equation must be tensors of the same rank. Stress and strain are tensors of rank 2. If the fibrous protein changes in the cells are related to stress and strain, then in a constitutive equation the fibrous protein changes must be stated also in tensor language. The molecular configuration tensor P_{ij}^g is a second order tensor. Every molecular configuration tensor P_{ij}^g has 9 components. The P_{31} and P_{32} values in the P_{ij}^g tensor of F-actin fiber in the individual vascular endothelial cells determined in this paper are related by the characteristic law [17].

In a theory to study the interrelation between the mechanical loading condition and remodeling of trabecular bone, Cowin defined a fabric tensor to characterize the arrangement of the microstructural components in a multiphasic or porous material [18]. Olsen et al. presented a model to study stress-induced alignment of matrix fibers [19]. Barocas and Tranquillo presented an anisotropic biphasic theory to account for traction-induced matrix reorganization within compacting tissue equivalents, in which an anisotropy tensor was used [20-21]. Nevertheless, their theories did not account for the geometrical arrangement of cellular molecules. Clearly, the biomechanics of tissue remodeling needs new input at the molecular level for expressing the mechanics of the molecules in a constitutive equation of the cells, which relates the stress, strain, molecular configuration, and their history. To accomplish this goal, the first step is to obtain the geometric information on the molecules. In the present paper, the molecular configuration tensorP_{ij}^g is defined to quantitatively describe the geometrical arrangement of fibrous proteins in the cells.

Summary. In conclusion, a second order *molecular configuration tensor* P_{ij}^g is defined to describe the geometric arrangement of fibrous proteins in the cells. The values of P_{31} and P_{32} in the P_{ij}^g tensor of F-actin fibers in the vascular endothelial cells were obtained and presented. The presented work provides a motivating investigation on the feasibility of the P_{ij}^g tensor used to describe the geometry of the cellular molecules in the cells and tissues.

Acknowledgement: This study was supported by the National Heart, Lung, and Blood Institute Grant HL- 43026, the National Foundation of Science Grant CMS-0626438, and by the University of California at San Diego Common Molecular Biochemistry Facility and Microscopy Facility, sponsored by the Whitaker foundation.

References

[1]**Chien, S.** (2007) *Am J Physiol Heart Circ Physiol.* 292, 1209-1224.

[2]**Nerem, R. M.; Levesque, M. J.; Cornhill, J. F.** (1981): *J Biomech Eng.* 103, 172-176.

[3]**DeBakey, M. E.; Lawrie, G. M.; Glaeser, D. H.** (1985): *Ann Surg.* 201, 115-131.

[1]**Giddens, D. P.; Zarins, C. K.,; Glagov, S.** (1993): *J Biomech Eng.* 115, 588-594.

[2]**Helmke, B. P.; Goldman, R. D.; Davies, P. F.** (2000): *Circ Res* 86, 745-752.

[3]**Karlon, W. J.; Hsu, P. P.; Li, S.; Chien, S.; McCulloch, A. D.; Omens, J. H.** (1999): *Ann Biomed Eng* 27, 712-720.

[4]**Langille, B. L.; Graham, J. J.; Kim, D.; Gotlieb, A. I.** (1991): *Arterioscler Thromb* 11, 1814-1820.

[5]**Sipkema, P.; van der Linden, P. J.; Westerhof, N.; Yin, F. C.** (2003): *J Biomech* 36, 653-659.

[6]**Kaunas, R.; Nguyen, P.; Usami, S.; Chien, S.** (2005): *Proc Natl Acad Sci U S A* 102, 15895-15900.

[7]**Hu, S.; Chen, J.; Fabry, B.; Numaguchi, Y.; Gouldstone, A.; Ingber, D. E.; Fredberg, J. J.; Butler, J. P.; Wang, N.** (2003): *Am J Physiol Cell Physiol* 285, C1082-C1090.

[8]**Mofrad, R. K.; Kamm, R. D.** (Eds.) (2006): *Cytoskeletal Mechanics: models and measurements.* Cambridge University Press, 244 pages, New York, NY.

[9]**Adams, A. E. M.; Pringle, J. R.** (1991): *Meth Enzym* 194, 729-731.

[10]**Bink, K.; Walch, A.; Feuchtinger, A.; Eisenmann, H.; Hutzler, P.; Höfler, H.; Werner, M.** (2001): *Histochem Cell Biol* 115, 293-299.

[11]**Galbraith, C. G.; Skalak, R.; Chien, S.**: (1998) *Cell Motil Cytoskeleton* 40, 317-330.

[12]**Fung, Y. C.** (1993): *Biomechanics: Mechanical Properties of Living Tissues*, 2nd ed., Springer-Verlag, 568 pages, New York, NY.

[13]**Humphrey, J.** (1999): *J. Biom. Engin* 121, 259-262.

[14]**Fung, Y. C.** (1994): *A First Course in Continuum Mechanics: for Physical and Biological Scientists and Engineers*, 3rd edition. Prentice-Hall, New Jersey, pp. 55-57.

[15]**Cowin, S. C.** (1985): *Mechanics Mater.* 4, 137-147.

[16]**Olsen, L.; Maini, P. K.; Sherratt, J. A.; Dallon, J. C.** (1999): *Math. Biosci.* 158, 145-170.

[17]**Barocas, V. H.; Tranquillo, R. T.** (1997): *J. Biomech. Eng.* 119, 137-145.

[18]**Barocas, V. H.; Tranquillo, R. T.** (1997): *J. Biomech. Eng.* 119, 261-268.